Article

Controlling Matter-Wave Smooth Positons in Bose–Einstein Condensates

Kannan Manikandan [1] , Nurzhan Serikbayev [2,3,*], Shunmuganathan P. Vijayasree [4] and Devarasu Aravinthan [1]

[1] Center for Computational Modeling, Chennai Institute of Technology, Chennai 600 069, Tamilnadu, India; manikandank@citchennai.net or manikandan.cnld@gmail.com (K.M.); aravinthand@citchennai.net (D.A.)
[2] Department of General and Theoretical Physics, L. N. Gumilyov Eurasian National University, Astana 010008, Kazakhstan
[3] Laboratory for Theoretical Cosmology, International Center of Gravity and Cosmos, Tomsk State Univerity of Control Systems and Radio Electronics (TUSUR), 634050 Tomsk, Russia
[4] Department of Computer Science and Engineering, Chennai Institute of Technology, Chennai 600 069, Tamilnadu, India; vijayasreeshunmuganathan@gmail.com
* Correspondence: serikbayev_ns@enu.kz

Abstract: In this investigation, we explore the existence and intriguing features of matter-wave smooth positons in a non-autonomous one-dimensional Bose–Einstein condensate (BEC) system with attractive interatomic interactions. We focus on the Gross–Pitaevskii (GP) equation/nonlinear Schrödinger-type equation with time-modulated nonlinearity and trap potential, which govern nonlinear wave propagation in the BEC. Our approach involves constructing second- and third-order matter-wave smooth positons using a similarity transformation technique. We also identify the constraints on the time-modulated system parameters that give rise to these nonlinear localized profiles. This study considers three distinct forms of modulated nonlinearities: (i) kink-like, (ii) localized or sech-like, and (iii) periodic. By varying the parameters associated with the nonlinearity strengths, we observe a rich variety of captivating behaviors in the matter-wave smooth positon profiles. These behaviors include stretching, curving, oscillating, breathing, collapsing, amplification, and suppression. Our comprehensive studies shed light on the intricate density profile of matter-wave smooth positons in BECs, providing valuable insights into their controllable behavior and characteristics in the presence of time-modulated nonlinearity and trap potential effects.

Keywords: matter waves; positons; Bose–Einstein condensates; Gross–Pitaevskii equation; similarity transformation

1. Introduction

Theoretical investigations into the nonlinear collective excitations of matter waves have emerged as a highly intriguing and pertinent field, especially in light of the experimental observations of Bose–Einstein condensation (BEC) in vapors of alkali metal atoms [1,2]. Among the captivating manifestations of localized waves in atomic matter, solitons inspire particular interest. The concept of a soliton was initially introduced to describe nonlinear solitary waves that exhibit remarkable properties, such as non-dispersive behavior, preserving their localized form and speeds both during propagation and after collisions [3–9]. These inherent advantages of solitons have sparked significant interest in the study of nonlinear systems across various fields of physics, particularly in high-rate telecommunications involving optical fibers, fluid dynamics, capillary waves, hydrodynamics, plasma physics, and so on [4,6,10–12]. On the other hand, BECs emit Faraday and resonant density waves when subjected to harmonic driving [13]. The characteristics of density waves in dipolar condensates at a temperature of absolute zero have been investigated using both mean-field variational and full numerical approaches [13]. The breaking of symmetry resulting from the anisotropy of the dipole–dipole interaction was found to be a crucial factor in this phenomenon.

From an experimental perspective, precise control over the existence of matter waves in a BEC system can be achieved by effectively manipulating nonlinear atom interactions using the Feshbach resonance (FR) technique as well as by varying the external trap potential [14–17]. This flexibility permits us to consider that the coefficient of nonlinearity and the external potential terms in the Gross–Pitaevskii (GP) equation/generalized nonlinear Schrödinger (NLS) equation can vary as functions of both time and/or space. Consequently, investigating the distinctive features of matter waves (solitons, breathers, and rogue waves) becomes highly intriguing given their spatial and temporal localization, particularly in the context of BEC experiments. Motivated by these achievements, extensive research has been dedicated to investigating localized matter waves within quasi-one-dimensional BECs [17–24]. Furthermore, studies focusing on the variable coefficient NLS equation have unveiled the possibility of manipulating and enhancing these localized profiles through the utilization of inhomogeneity parameters [5–7,25–31]. Moreover, investigations have explored the identification of soliton solutions in the generalized NLS equation with spatially modulated parameters and an external potential [32–35]. Notably, in [32], the authors identified alternate solitons and determined their stability regions in both two-dimensional and one-dimensional BEC models. These investigations were conducted in the presence of optical lattices created by laser beams illuminating the condensates. The analysis of soliton propagation in optical and condensed matter systems with parity-time ($\mathcal{PT}$) symmetry, particularly in inhomogeneous setups, has received significant attention. Accordingly, considerable efforts have been devoted to showcasing the existence of stable bright solitons, dark solitons, and vortices within the NLS equation featuring $\mathcal{PT}$-symmetric potentials [36–38]. In the case of weakly interacting toroidal BECs, the occurrence of rotational fluxons (commonly known as Josephson vortices) is linked to the spontaneous disruption of the rotational symmetry within the tunneling superflows [39]. To explore the impact of controllable symmetry breaking on the resulting state of merged counter-propagating superflows, a weakly dissipative mean-field model was employed. In line with this research trajectory, our aim is to construct an intriguing type of localized solution known as smooth positons within the GP equation. We further endeavor to explore the effects of the time-dependent modulation of nonlinearity parameters on the characteristics of smooth positon profiles.

Positons, unlike exponentially decaying soliton solutions, are weakly localized nonlinear waves that hold significant importance in the field of nonlinear physics [40–43]. These solutions are obtained by constraining degenerate eigenvalues within the widely recognized N-soliton algorithm. For positon solutions, the corresponding eigenvalue in the spectral problem is positive and lies within the continuous spectrum. It has been observed that when two positons collide, they retain their individual identities, whereas a soliton remains unchanged following a collision with a positon. However, the positon is influenced by the carrier wave and envelope, resulting in a finite phase shift [44,45]. Notably, Matveev's positon solution to the Korteweg–de Vries (KdV) equation exhibited a spectral singularity [42]. Building on this pioneering work, positon solutions have been successfully derived for other nonlinear evolution equations; one may refer to [46–48] for more information. Recent efforts by Cen et al. introduced the concept of smooth positons or degenerate soliton solutions by allowing for the spectral parameter to take complex values [49,50], thereby eliminating the singularity in the KdV equation. Following these advancements, endeavors have been made to construct smooth positon solutions for various nonlinear evolution equations, including the focusing mKdV equation [51], the complex mKdV equation [52], the derivative NLS equation [53,54], the NLS–Maxwell–Bloch equation [55], the higher-order Chen–Lee–Liu equation [56], and the Gerdjikov–Ivanov equation [57]. More recently, smooth positons and breather positons have been derived for the generalized NLS equation with higher-order nonlinearity along with higher-order solutions for an extended NLS equation featuring cubic and quartic nonlinearity [58,59]. Inspired by these advancements in the field of positons, our research aims to construct

smooth positon solutions within the GP equation, incorporating time-varying nonlinearity and trap potentials.

The crucial step in this attempt involves utilizing a similarity transformation [5–8,20] on a meticulously chosen ansatz solution. This transformation effectively converts the GP equation with time-varying coefficients into the conventional NLS equation with constant coefficients. By implementing this transformation, the modified variables allow us to derive new solutions for the considered equation by expressing the known smooth positon solutions in the altered coordinate system [6,8,20,23]. By leveraging the combination of known positon solutions of typical NLS equations with similarity transformation functions, one can derive novel (non-autonomous positon) solutions for the GP equation. The integrability requirements, which establish the relationship between variable parameters (modulated nonlinearity and trap potentials), and the proposed ansatz solution, serve as the underlying considerations for this procedure. However, despite the associated costs, this approach holds significant value as it not only reveals new analytical solutions for the GP equation but also empowers users to control outcomes by judiciously selecting appropriate nonlinearity strengths and trap potentials [20,25,26].

Motivated by the experimental feasibility of studying BECs, our research focuses on exploring the characteristics of matter-wave smooth positons. To achieve this objective, we construct second- and third-order matter-wave positon solutions for the one-dimensional GP equation, considering a variable nonlinearity parameter and an external trap potential. The construction of these solutions involves transforming the time-modulated GP equation into a constant coefficient NLS (ccNLS) equation using a similarity transformation. We establish that the trapping potential and nonlinearity-modulated parameter must satisfy a constraint for the considered equation to be integrable and yield the desired solutions. By leveraging the known smooth positon solutions (second- and third-order) of the ccNLS equation, we present matter-wave smooth positon solutions of the GP equation. We investigate the controllable behavior of positon density profiles with respect to three different forms of variable nonlinearity parameters, namely, (i) kink-like nonlinearity $R(t) = R_0 + R_1 \tanh(R_2 t + R_3)$, (ii) localized or sech-type nonlinearity $R(t) = R_0 + R_1 \operatorname{sech}(R_2 t + R_3)$, and (iii) periodic nonlinearity $R(t) = R_0 + R_1 \sin(R_2 t + R_3)$, for which R_0, R_1, R_2 and R_3 are arbitrary parameters. Our findings reveal that a range of nonlinear physical phenomena, including stretching, curving, annihilation, breathing, oscillating, enhancement, and suppression, are manifested in the underlying matter-wave positon density profiles. When considering a kink-like modulated nonlinearity, the matter-wave positon density profiles of a second- and third-order experience stretching, while their amplitudes can either be enhanced or suppressed. It is important to note that these profiles vanish at different time intervals, with disappearance occurring for $t < 0$ when the parameter R_2 assumes positive values and for $t > 0$ when R_2 takes negative values. In the case of a localized or sech-type modulated nonlinearity, the positon density profiles become compressed and curved within the background density of the condensate. For periodic modulated nonlinearity, positons exhibit a periodic behavior, and adjusting the strengths of nonlinearity leads to an increase in their periodicity, as observed in our analysis. This observation provides valuable insights for experimentalists analyzing novel density profiles in BECs.

We have structured our work as follows. In Section 2, we account for the GP equation with time-modulated nonlinearity and trap potentials. The second and third-order smooth positon solutions are deduced for this equation using a similarity transformation. The integrability requirement between the modulated nonlinearity and trap potential is obtained while applying the integrable technique to the considered equation. In Section 3, by suitably choosing the different forms of the variable nonlinearity parameter, we explore the various characteristics in the density of matter-wave smooth positon profiles. Finally, in Section 4, we provide conclusions based on our observations.

2. BEC Model and Similarity Transformation

The behavior of a BEC confined within an external potential can be effectively characterized using the renowned NLS equation derived from mean field theory, which is commonly referred to as the GP equation. In the specific scenario of a cigar-shaped trapping potential, where simplicity and physical significance coincide, the radial degree of freedom in the three-dimensional GP equation can be eliminated through integration, leading to the derivation of a dimensionless quasi-one-dimensional equation [1,2,8,17,20]

$$i\frac{\partial\psi}{\partial t} + \frac{1}{2}\frac{\partial^2\psi}{\partial x^2} + R(t)|\psi|^2\psi + \frac{1}{2}\lambda^2(t)x^2\psi = 0, \tag{1}$$

where $\psi(x,t)$ is the condensate wave function and t and x represent dimensionless temporal (propagation direction) and spatial (transverse) coordinates, respectively. The atom–atom interaction term (i.e., the scattering length between atoms) denoted by the representation, $R(t)$, can be tuned using the FR technique. In a series of exquisite experiments using sodium and rubidium condensates, FRs were investigated [14,15]. They have also been employed in a variety of significant experimental studies, such as the creation of bright and dark matter-wave solitons, among others. The time-modulated trap potential is denoted by $\lambda^2(t)$. In the study of trapped BECs, the trap potential along the elongated axis has been intentionally selected to vary with time, t, in order to investigate the characteristics of the BECs within the trap. As a result, both the coefficient of nonlinearity (R) and the potential parameter (λ) can exhibit time dependence. By appropriately selecting these two time-dependent parameters, the GP Equation (1) can effectively capture the dynamics and manipulation of BECs. These parameters serve as powerful tools for controlling and manipulating localized matter waves in BECs, which can be achieved through the adjustment of external magnetic fields and optically controlled interactions using techniques such as the FR method [16,20,23]. It is worth noting that such an analysis can be extended to study the influence of space-dependent parameters on solitons/positons in the system under consideration (1) or in the context of the generalized NLS equation with the presence of optical lattices. A noteworthy and unique characteristic of solitons in the presence of nonlinear lattices is the existence of a finite threshold value of the soliton norm, which is necessary for the lattices' formation [32]. This property does not occur in the absence of nonlinear lattices. In nonlinear lattices, solitons are created directly as opposed to bifurcating from Bloch modes as seen in linear lattices. This distinction highlights the unique nature and behavior of solitons in the presence of spatially modulated nonlinearity [32,33]. As a consequence of these observations, substantial progress have been made with regard to investigating the localized solutions in the generalized NLS equation with spatially modulated parameters and the external potential [32–35]. This opens up promising avenues for future investigations with respect to understanding the behavior and dynamics of solitons and positons in spatially modulated systems.

In this work, to study the matter-wave smooth positons in (1), we adopt the similarity transformation mentioned below to map the time-modulated GP Equation (1) to the ccNLS equation [5–8,20,38]:

$$\psi(x,t) = s(t)\phi(\eta(x,t),\tau(t))\exp[i\theta(x,t)]. \tag{2}$$

In Equation (2), the unknown functions, namely, $s(t), \eta(x,t), \tau(t)$, and $\theta(x,t)$, are the amplitude, similarity spatial variable, the dimensionless time, and the phase factor, respectively, which are to be computed. Upon involving the substitution of (2) into (1), we obtain the following set of partial differential equations that are related to the unknown functions:

$$\eta_{xx} = 0, \tag{3a}$$

$$\eta_t + \eta_x\theta_x = 0, \tag{3b}$$

$$\eta_x^2 - R(t)s^2(t) = 0, \tag{3c}$$

$$s'(t) + s(t)\frac{1}{2}\theta_{xx} = 0, \tag{3d}$$

$$\tau'(t) - R(t)s^2(t) = 0, \tag{3e}$$

$$\theta'(t) + \frac{1}{2}\theta_x^2 - \frac{\lambda^2(t)}{2}x^2 = 0. \tag{3f}$$

The explicit expressions of the unknown functions can be acquired by solving the aforementioned set of equations, and they take the following form

$$s(t) = s_0\sqrt{R(t)}, \tag{4a}$$

$$\eta(x,t) = s_0 R(t)x - bs_0^3 \int R^2(t)dt, \tag{4b}$$

$$\theta(x,t) = -\frac{R(t)_t}{2R(t)}x^2 + bs_0^2 R(t)x - \frac{1}{2}b^2 s_0^4 \int R^2(t)dt, \tag{4c}$$

$$\tau(t) = \frac{1}{2}s_0^2 \int R^2(t)dt. \tag{4d}$$

where b and s_0 are arbitrary constants. Additionally, we have found an integrability condition that imposes a connection between the time-modulated nonlinearity and the trap potential parameter, as shown in [8,20,38].

$$\frac{d}{dt}\left(\frac{R_t}{R}\right) - \left(\frac{R_t}{R}\right)^2 + \lambda^2(t) = 0. \tag{5}$$

Using Equation (5), one can find the $\lambda(t)$ by fixing the $R(t)$, and vice versa. In this work, we consider the physically intriguing function $R(t)$ and determine the $\lambda(t)$ via the following expression: $\lambda(t) = \dfrac{\sqrt{R'(t)^2 + R'(t) - R(t)R''(t)}}{R(t)}$.

In Equation (2), the function $\phi(\eta, \tau)$ was found to fulfill the ccNLS equation:

$$i\frac{\partial\phi}{\partial\tau} + \frac{1}{2}\frac{\partial^2\phi}{\partial\eta^2} + |\phi|^2\phi = 0. \tag{6}$$

The equation under consideration (6) exhibits a wide range of localized solutions, including solitons, breathers, rogue waves, and their corresponding profiles [6,20,43]. In this study, we focus on the smooth positon solutions of the NLS equation to investigate matter-wave positons in quasi-one-dimensional BECs.

By selecting an appropriate functional form for the time-modulated nonlinearity function $R(t)$ while ensuring the satisfaction of condition (5), we can derive matter-wave positon solutions for the GP Equation (1) in the following form:

$$\psi(x,t) = s_0\sqrt{R(t)}\phi(\eta, \tau)\exp\left[i\left(-\frac{1}{2}b^2 s_0^4\int R(t)^2\,dt + bs_0^2 xR(t) - \frac{x^2 R'(t)}{2R(t)}\right)\right], \tag{7}$$

where $\phi(\eta, \tau)$ is the smooth positon solution of the ccNLS Equation (6). The solution (7) has the potential to generate a multitude of novel positon structures that can be experimentally realized. To summarize the current progress, one can generate several solutions (positons) for the GP model (1) by first obtaining solutions for the ccNLS Equation (6) while satisfying the mentioned relationships. An intriguing advantage of and potential new perspective regarding the similarity transformation is worth emphasizing, as it allows for the extension of this approach to models featuring variable nonlinearity and external trap potential coefficients dependent on both longitudinal and spatial coordinates. By appropriately tailoring and imposing constraints, the resulting dynamics of physical systems can be attainable. Consequently, in Section 3, we construct smooth positon solutions for the ccNLS Equation (6) to analyze matter-wave positons in quasi-one-dimensional BECs.

3. Characteristics of Matter-Wave Smooth Positons in BECs

In this section, we investigate the characteristics of matter-wave positons using solution (7) by considering three different forms of the time-varying nonlinearity parameter and the associated trap potentials. For this investigation, in the following, we first derive the second-order and third-order smooth positon solution for the ccNLS Equation (6).

3.1. Second-Order Matter-Wave Smooth Positons

Now, we explore the various novel density profiles of second-order matter-wave smooth positons in BECs. For this objective, we first derive the second-order smooth positon solution for the ccNLS Equation (6) as provided by

$$\phi[2] = \frac{P_{11}}{Q_{11}}, \tag{8}$$

where

$$
\begin{aligned}
P_{11} =& 4(\alpha_1 - \alpha_1^*)e^{2i\alpha_1(2\alpha_1\tau+\eta)}\left(-\alpha_1(\eta - 4\alpha_1^*\tau) + \alpha_1^*\eta - 4\alpha_1^2\tau - i\right) \\
&+ 4(\alpha_1^* - \alpha_1)e^{2i\alpha_1^*(2\alpha_1^*\tau+\eta)}\left(-\alpha_1(4\alpha_1^*\tau + \eta) + \alpha_1^*\eta + 4(\alpha_1^*)^2\tau + i\right),
\end{aligned} \tag{9a}
$$

$$
\begin{aligned}
Q_{11} =& -2e^{\left(2i(\alpha_1+\alpha_1^*)\eta + 4i(\alpha_1^2+\alpha_1^{*2})\tau\right)}\left(-1 + 2(\alpha_1 - \alpha_1^{*2})\eta^2 + 32\alpha_1\alpha_1^*(\alpha_1 - \alpha_1^*)^2\tau^2 \right. \\
&\left. + 8\eta\tau(\alpha_1 + \alpha_1^*)(\alpha_1 - \alpha_1^{*2})\right) + e^{4i\alpha_1(2\alpha_1\tau+\eta)} + e^{4i\alpha_1^*(2\alpha_1^*\tau+\eta)},
\end{aligned} \tag{9b}
$$

where α_1 is the eigenvalue of the spectral parameter, α_1^* is the complex conjugate of α_1, and η and τ are provided in Equation (4). The above-mentioned second-order smooth positon solution (8) can be obtained from the material presented in [58] by considering $\nu = 0$. Substituting this solution into (7) along with the suitable form of $R(t)$, we obtain the second-order matter-wave smooth positon solution of (1).

Now, utilizing the above mentioned solution, we move to investigate its controllable behaviors through three different forms of a time-modulated nonlinearity parameter, namely, (i) kink-like nonlinearity $R(t) = R_0 + R_1 \tanh(R_2 t + R_3)$, (ii) localized or sech-type nonlinearity $R(t) = R_0 + R_1 \operatorname{sech}(R_2 t + R_3)$, and (iii) periodic nonlineaity $R(t) = R_0 + R_1 \sin(R_2 t + R_3)$, where R_0, R_1, R_2, and R_3 are arbitrary parameters. Moreover, it is important to mention that this investigation can be extended to study the impact of spatially modulated coefficients [32–35] on the matter-wave smooth positons of (1), which will provide fruitful directions for future investigations. In the following, we provide a comprehensive demonstration of the impact of time-modulated nonlinearity parameters on the positon density profiles.

To begin, we employ the kink-like nonlinearity parameter, that is, $R(t) = R_0 + R_1 \tanh(R_2 t + R_3)$, to reveal the novel features in BECs. Substituting this nonlinearity term into the generalized solution (7) yields

$$
\begin{aligned}
\psi(x,t) =& s_0\sqrt{R_1\tanh(R_2 t + R_3) + R_0}\,\phi(\eta,\tau)\exp\left[-\frac{i}{4R_2}\left(b^2 s_0^4\left(-2R_1^2\right.\right.\right. \\
&\times \tanh(R_2 t + R_3) + (R_0 - R_1)^2\log(\tanh(R_2 t + R_3) + 1) - (R_0 + R_1)^2 \\
&\times \log(1 - \tanh(R_2 t + R_3))) - 4bs_0^2 x(R_1\tanh(R_2 t + R_3) + R_0) \\
&\left.\left.\left.+\frac{2R_1 R_2 x^2\operatorname{sech}^2(R_2 t + R_3)}{R_1\tanh(R_2 t + R_3) + R_0}\right)\right],
\end{aligned} \tag{10}
$$

where $\phi(\eta,\tau)$ is the second-order smooth positon solution of the ccNLS Equation provided in Equation (8). Utilizing this solution (10), we conduct a thorough analysis of the positon density profiles, investigating their diverse characteristics as we vary the strength of the time-modulated nonlinearity parameter.

　　　Figure 1a–f illustrate the qualitative profiles of a second-order matter-wave smooth positon in BECs corresponding to a kink-like nonlinearity modulated parameter $R(t) = R_0 + R_1 \tanh(R_2 t + R_3)$. By selecting specific parameter values, i.e., $R_0 = 1.05$, $R_1 = 0.01$, $R_2 = 1.05$, and $R_3 = 0.5$, we obtain a well-localized second-order smooth positon profile associated with the eigenvalue $\alpha_1 = 0.2 + 0.5i$, as depicted in Figure 1a. Notably, the orientation of the smooth positon density profile changes when varying the eigenvalue associated with the solution. For instance, when modifying the eigenvalue to $\alpha_1 = 0.3 + 0.6i$, Figure 1b clearly demonstrates a shift in the orientation of the positon profile accompanied by an enhancement of its amplitude. Furthermore, we investigate the effects of adjusting the strengths of the nonlinearity parameters, specifically R_0, R_1, and R_2. For example, when R_0 is changed to 1.85, the positon profile's orientation relocates while experiencing a slight increase in amplitude, as depicted in Figure 1c. Additionally, Figure 1d illustrates that increasing the value of R_1 to 0.5 leads to the collapse of the condensate profile on one side of the positon profile ($t < 0$). Conversely, when R_1 assumes a negative value, such as $R_1 = -0.5$, the reverse phenomenon occurs, resulting in the disappearance of the density profile in the corresponding plane ($t > 0$) as represented in Figure 1e. Moreover, increasing the value of R_2 to 3.5 yields a well-localized positon profile that exhibits a compression within the condensate density background. Additionally, as depicted in Figure 1f, the width of the crest of the positon profile widens over time.

　　　Next, we consider localized-type or sech-type nonlinearity, namely, $R(t) = R_0 + R_1$ sech $(R_2 t + R_3)$, in order to investigate the distortion of positon profiles in the condensate density background. By inserting this form of $R(t)$ into (7), we obtain the matter positon solution in the following form

$$
\begin{aligned}
\psi(x,t) = \; & s_0 \sqrt{R_1 \text{sech}(R_2 t + R_3) + R_0}\, \phi(\eta,\tau) \exp\left[\frac{i}{2R_2} \left(-b^2 s_0^4 \left(R_2 R_0^2 t \right. \right. \right. \\
& \left. + R_1^2 \tanh(R_2 t + R_3) + 2 R_1 R_0 \tan^{-1}(\sinh(R_2 t + R_3)) \right) \\
& \left. \left. + b s_0^2 x (R_1 \text{sech}(R_2 t + R_3) + R_0) + \frac{R_1 R_2 x^2 \tanh(R_2 t + R_3)}{2(R_0 \cosh(R_2 t + R_3) + R_1)} \right) \right],
\end{aligned}
\tag{11}
$$

where $\phi(\eta, \tau)$ is the positon solution of the ccNLS Equation, which is provided in Equation (8).

　　　Figure 2a–f represent the density profiles of a second-order matter-wave smooth positon with a modulated nonlinearity function yielded by $R(t) = R_0 + R_1$ sech $(R_2 t + R_3)$. In this study, we consider specific parameter values, i.e., $R_0 = 1.05$, $R_1 = 0.01$, $R_2 = 1.05$, and $R_3 = 0.5$, aiming to investigate the intriguing properties exhibited by the positon density profiles. With these initial parameter values, we obtain the second-order smooth positon profile, as shown in Figure 2a. By increasing R_0 to 1.85, we observe a stretching of the positon and an enhancement in its amplitude, as depicted in Figure 2b. Similarly, when we tune the parameter R_1 to 0.85, a curvature appears in the condensate profile, as shown in Figure 2c. Notably, when R_1 assumes a negative value, we observe the formation of two peaks at the center ($t = 0$), which is accompanied by a suppression in amplitude, as demonstrated in Figure 2d. Additionally, in the case where $R_0 = 1.85$ and $R_1 = 1.75$, we observe a gradual increase in amplitude, the further stretching of the positon, and the formation of a curved profile, as shown in Figure 2e. At $R_0 = 2.5$ and $R_2 = 1.5$, a compressed density profile with an identical amplitude is obtained, as depicted in Figure 2f.
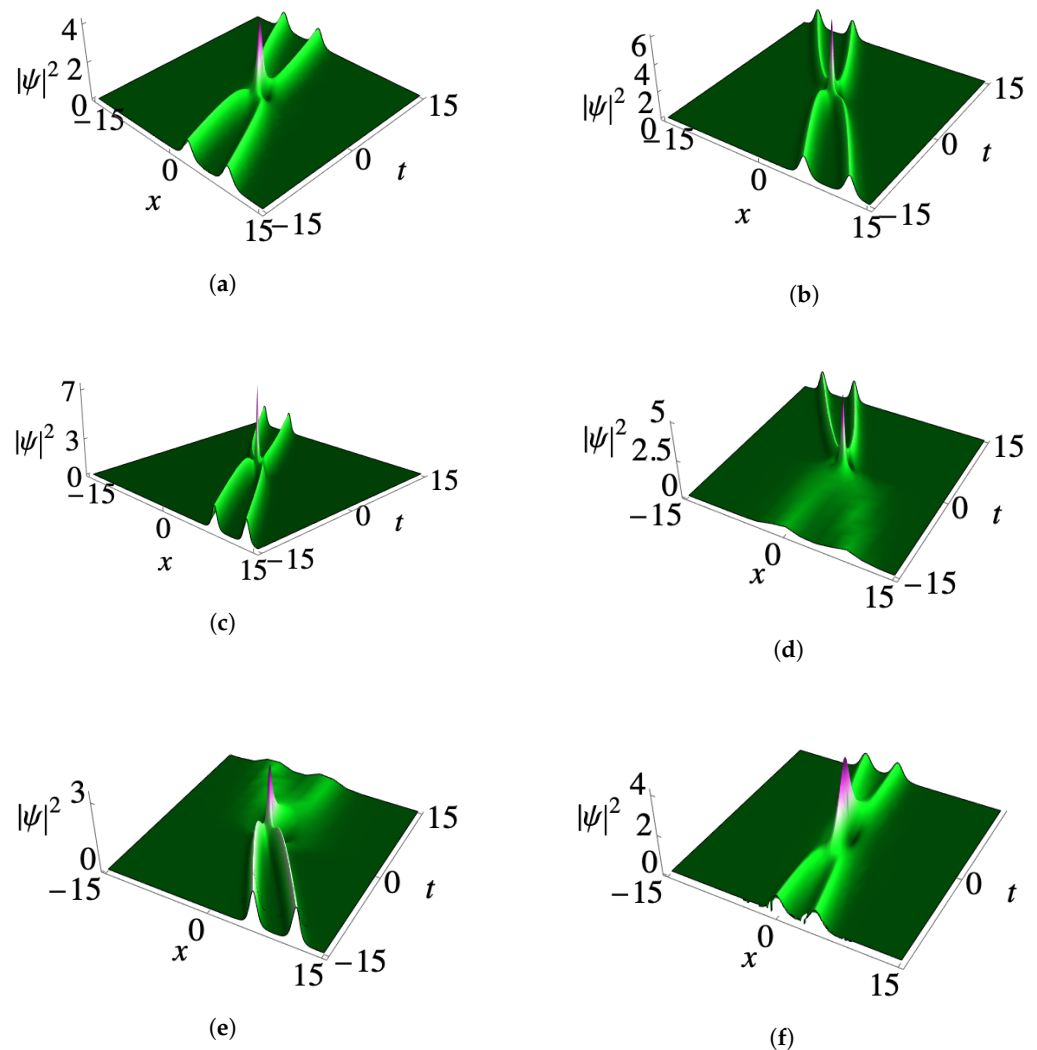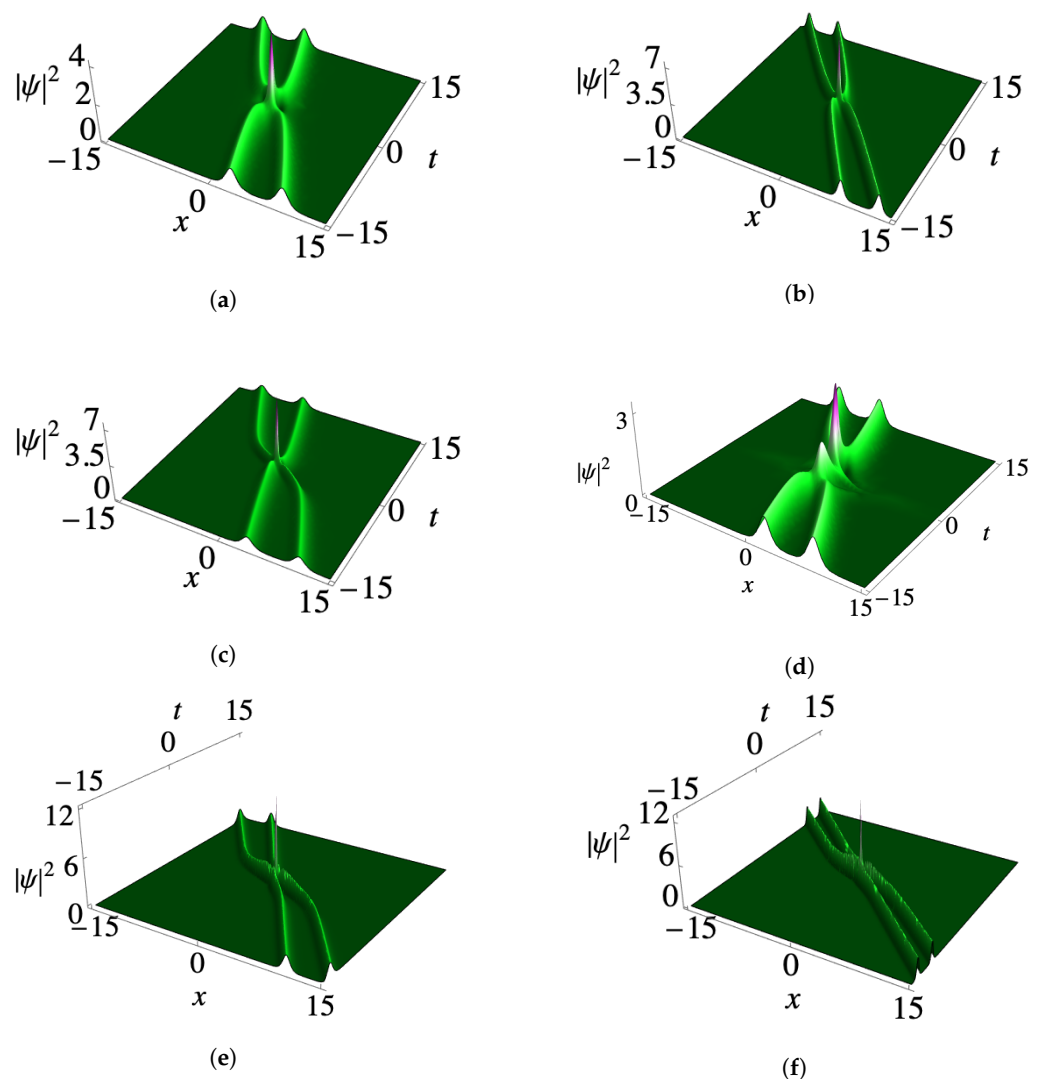
Figure 1. Density profile of second-order matter-wave smooth positons for (1) with the kink-like nonlinearity modulated function $R(t) = R_0 + R_1 \tanh(R_2 t + R_3)$. The parameters are (**a**) $R_0 = 1.05$, $R_1 = 0.01$, $R_2 = 1.05$, $R_3 = 0.5$; (**b**) $\alpha_1 = 0.3 + 0.6i$, $\alpha_1^* = 0.3 - 0.6i$; (**c**) $R_0 = 1.85$; (**d**) $R_1 = 0.5$; (**e**) $R_1 = -0.5$; (**f**) $R_2 = 3.5$. In (**b**–**f**), the mentioned parameters are varied, while the remaining parameters are maintained as they are in (**a**). The other parameters are $\alpha_1 = 0.2 + 0.5i$, $\alpha_1^* = 0.2 - 0.5i$, $s_0 = 1.0$, and $b = 0.01$.

Finally, we investigate the influence of a periodically modulated nonlinearity given by $R(t) = R_0 + R_1 \sin(R_2 t + R_3)$ on the positon density profiles. By inserting this $R(t)$ into (7), we obtain the explicit form of a matter-wave positon solution yielded in the following expression:

$$
\begin{aligned}
\psi(x,t) =\, & s_0 \sqrt{R_1 \sin(R_2 t + R_3) + R_0}\, \phi(\eta, \tau) \exp\left(-\frac{i}{8R_2}\left(b^2 s_0^4\left(4R_0^2(R_2 t + R_3)\right.\right.\right. \\
& + R_1^2(2R_2 t - \sin(2(R_2 t + R_3)) + 2R_3) - 8R_1 R_0 \cos(R_2 t + R_3)\big) \\
& \left.\left.- 8bs_0^2 x(R_1 \sin(R_2 t + R_3) + R_0) + \frac{4R_1 R_2 x^2 \cos(R_2 t + R_3)}{R_1 \sin(R_2 t + R_3) + R_0}\right)\right),
\end{aligned}
\tag{12}
$$

where $\phi(\eta, \tau)$ is the positon solution of the ccNLS Equation given in (8).

The second-order matter-wave smooth positon density profiles are displayed in Figure 3 for a periodic nonlinearity-modulated function $R(t) = R_0 + R_1 \sin(R_2 t + R_3)$ in the context of BECs. By appropriately tuning the parameters R_0, R_1, and R_2, we can achieve periodic positon solutions. In Figure 3a, using initial parameter values of $R_0 = 1.5$, $R_1 = 0.05$, $R_2 = 1.25$, and $R_3 = 0.5$, we can observe a periodic behavior in the positon condensate profile. Subsequently, when the nonlinearity strength R_0 is increased to 2.25, the oscillation of the positon becomes more elongated, and the amplitude is raised, as shown in Figure 3b. Moreover, as we increase the value of R_1 to 0.55, the periodicity of the positon profile increases along with an increase in amplitude, which can be seen in Figure 3c. This trend is further amplified when the value of R_1 is increased, as depicted in Figure 3d. When the parameters $R_2 = 2.75$ and 5.25 are chosen, the oscillation in the positon profile increases and retains a similar orientation, as evident in Figure 3e,f, respectively.

Figure 2. Density profile of second-order matter-wave smooth positons for (1) with localized-type modulated nonlinearity $R(t) = R_0 + R_1 \operatorname{sech}(R_2 t + R_3)$. The parameters are (**a**) $R_0 = 1.05$, $R_1 = 0.01$, $R_2 = 1.05$, $R_3 = 0.5$; (**b**) $R_0 = 1.85$; (**c**) $R_1 = 0.85$; (**d**) $R_1 = -0.85$; (**e**) $R_0 = 1.85$, $R_1 = 1.75$; (**f**) $R_0 = 2.5$, $R_2 = 1.5$. In (**b**–**f**), the mentioned parameters are varied, while the remaining parameters are kept as they are in (**a**). The other parameters are the same as in Figure 1.
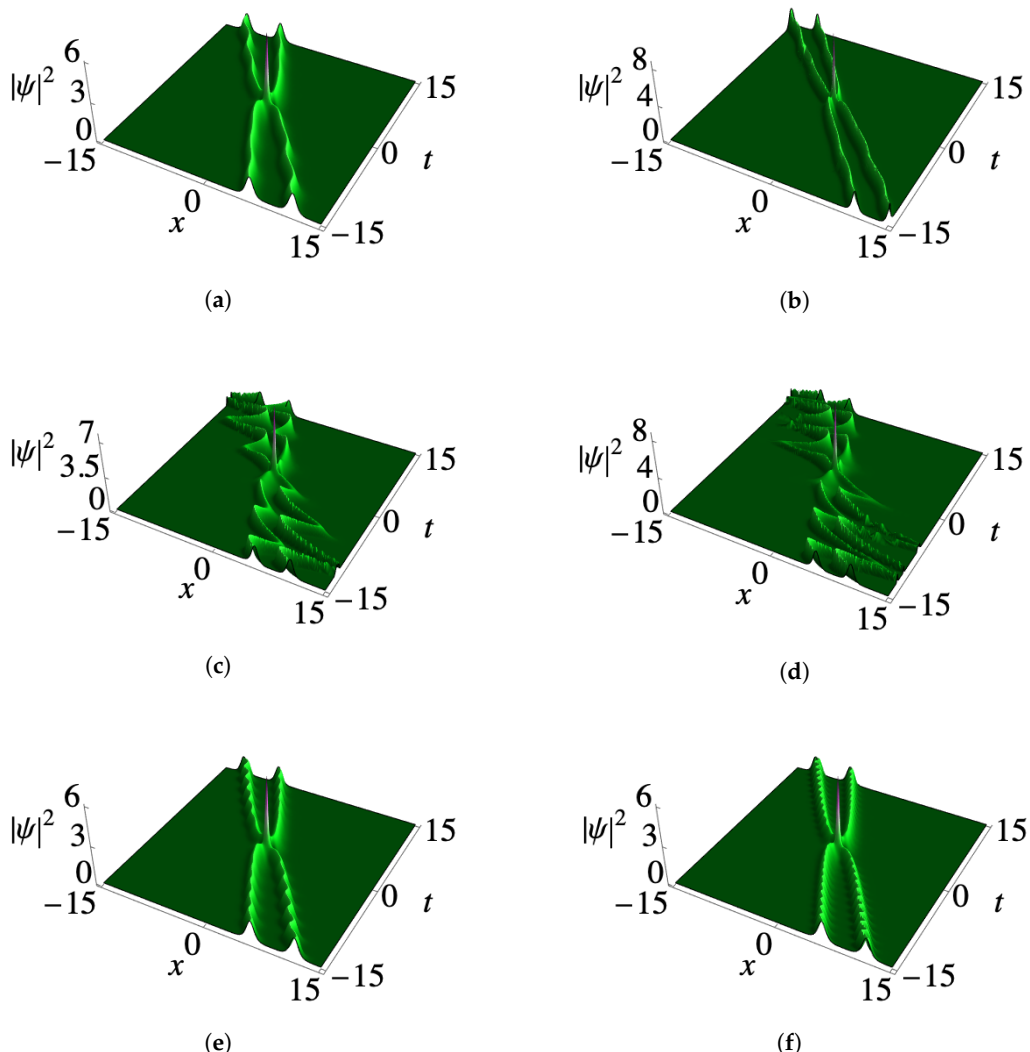
Figure 3. Density profile of second-order matter-wave smooth positons for (1) with the periodic nonlinearity modulated function $R(t) = R_0 + R_1 \sin(R_2 t + R_3)$. The parameters are (**a**) $R_0 = 1.5$, $R_1 = 0.05$, $R_2 = 1.25$, $R_3 = 0.5$; (**b**) $R_0 = 2.25$; (**c**) $R_1 = 0.55$; (**d**) $R_1 = 0.85$; (**e**) $R_2 = 2.75$; (**f**) $R_2 = 5.25$. In (**b**–**f**), the mentioned parameters are varied, while the remaining parameters are maintained as they are in (**a**). The other parameters are the same as in Figure 1.

3.2. Third-Order Matter-Wave Smooth Positons

In the previous sub-section, we investigated the modifications of second-order matter-wave smooth positon profiles by varying the distributed coefficients (the nonlinearity function) in the GP Equation (1). In this sub-section, we delve into the deformations of third-order matter-wave smooth positons in condensates as we manipulate the strength of the modulated nonlinearity parameter. To explore these intriguing characteristics, we consider the third-order smooth positon solution for the ccNLS Equation (6), which takes the following form:

$$\phi[3] = \frac{P_2}{Q_2},\tag{13}$$

where

$$P_2 = e^{-i\left(2\tau\left(\alpha_1^2 + \alpha_1^{*2}\right) + \eta\left(\alpha_1 + \alpha_1^*\right)\right)}\left(P_{21}e^{2i(\alpha_1 - \alpha_1^*)(\eta + 2\tau(\alpha_1 + \alpha_1^*))}\right.$$

$$\left. + P_{22}e^{-2i(\alpha_1 - \alpha_1^*)(\eta + 2\tau(\alpha_1 + \alpha_1^*))} + P_{23}\right),\tag{14}$$

with

$$
\begin{aligned}
P_{21} = &- 4(\alpha_1 - \alpha_1^*)\Big(-3 + 2\eta\,(3i + 8\tau\alpha_1(\alpha_1 - \alpha_1^*) + 2\eta^2(\alpha_1 - \alpha_1^*)^2 \\
&+ 32\tau^2\alpha_1^2(\alpha_1 - \alpha_1^*)^2 - 4i\tau(\alpha_1 - \alpha_1^*)(-7\alpha_1 + \alpha_1^*)\Big),
\end{aligned}
$$

$$
\begin{aligned}
P_{22} = &- 4(\alpha_1 - \alpha_1^*)\Big(-3 + 4i\tau(\alpha_1 - 7\alpha_1^*)(\alpha_1 - \alpha_1^*) + 2\eta^2(\alpha_1 - \alpha_1^*)^2 \\
&+ 32\tau^2(\alpha_1 - \alpha_1^*)^2\alpha_1^{*2} - 2\eta(\alpha_1 - \alpha_1^*)(3i + 8\tau\alpha_1^*(-\alpha_1 + \alpha_1^*))\Big),
\end{aligned}
$$

$$
\begin{aligned}
P_{23} = &\, 8(\alpha_1 - \alpha_1^*)\Big(3 + 4\eta^2(\alpha_1 - \alpha_1^*)^2 - 2\eta^4(\alpha_1 - \alpha_1^*)^4 + \alpha_1^2 - 512\tau^4\alpha_1^2(\alpha_1 - \alpha_1^*)^4\alpha_1^{*2} \\
&+ 8i\eta\alpha_1^{*3} - 4\eta^2\alpha_1^{*4} - 8\eta\alpha_1^3(-i + \eta\alpha_1^*) - 2\alpha_1\alpha_1^*(-3 + 4i\eta\alpha_1^* + 4\eta^2\alpha_1^{*2}) \\
&+ 16\tau(\alpha_1 - \alpha_1^*)^2(-i + i\eta^2(\alpha_1 - \alpha_1^*)^2 + \eta(\alpha_1 + \alpha_1^*) - \eta^3(\alpha_1 - \alpha_1^*)^2(\alpha_1 + \alpha_1^*)) \\
&+ 8\tau^3(\alpha_1 - \alpha_1^*)^3(\alpha_1 + \alpha_1^*)(-i\alpha_1^* + \alpha_1(-i + 4\eta\alpha_1^*)) \\
&+ 8\tau^2(\alpha_1 - \alpha_1^*)^2(\alpha_1^2 - 8i\eta\alpha_1^2\alpha_1^* + \eta^2(1 + 24\alpha_1^2\alpha_1^{*2}))\Big),
\end{aligned}
$$

and

$$
\begin{aligned}
Q_2 = &\, 4e^{-3i(\alpha_1 - \alpha_1^*) + (\eta + 2\tau(\alpha_1 + \alpha_1^*))}\Big(1 + Q_{21}e^{4i(\alpha_1 - \alpha_1^*)(\eta + 2\tau(\alpha_1 + \alpha_1^*))} \\
&+ Q_{22}e^{2i(\alpha_1 - \alpha_1^*)(\eta + 2\tau(\alpha_1 + \alpha_1^*))} + e^{6i(\alpha_1 - \alpha_1^*)(\eta + 2\tau(\alpha_1 + \alpha_1^*))}\Big),
\end{aligned}
\tag{15}
$$

where

$$
\begin{aligned}
Q_{21} = &\, 3 + 1024\tau^4\alpha_1^2(\alpha_1 - \alpha_1^*)^4\alpha_1^{*2} + 48\tau^2(\alpha_1 - \alpha_1^*)^2(\alpha_1^2 - 6\alpha_1\alpha_1^* + \alpha_1^{*2}) \\
&+ 4\eta^4(\alpha_1 - \alpha_1^*)^4 - 128i\tau^3(\alpha_1 - \alpha_1^*)^3(\alpha_1 + \alpha_1^*)(\alpha_1^2 - 4\alpha_1\alpha_1^* + \alpha_1^{*2}) \\
&+ 8\eta^3(\alpha_1 - \alpha_1^*)^3(i + 4\tau(\alpha_1^2 - \alpha_1^{*2})) + 4\eta^2(\alpha_1 - \alpha_1^*)^2\Big(-3 + 12i\tau(\alpha_1^2 - \alpha_1^{*2}) \\
&+ 16\tau^2(\alpha_1 - \alpha_1^*)^2(\alpha_1^2 + 4\alpha_1\alpha_1^* + \alpha_1^{*2}) - 16\eta\tau(\alpha_1 - \alpha_1^*)^2\Big(3\alpha_1^* - 32\tau^2\alpha_1^4\alpha_1^* \\
&+ 32\tau^2\alpha_1^3\alpha_1^{*2} + 8\tau\alpha_1^2\alpha_1^*(-3i + 4\tau\alpha_1^{*2}) + \alpha_1(3 + 24i\tau\alpha_1^{*2} - 32\tau^2\alpha_1^{*4})\Big),
\end{aligned}
$$

$$
\begin{aligned}
Q_{22} = &\, 3 + 1024\tau^4\alpha_1^2(\alpha_1 - \alpha_1^*)^4\alpha_1^{*2} + 48\tau^2(\alpha_1 - \alpha_1^*)^2(\alpha_1^2 - 6\alpha_1\alpha_1^* + \alpha_1^{*2}) \\
&+ 4\eta^4(\alpha_1 - \alpha_1^*)^4 + 128i\tau^3(\alpha_1 - \alpha_1^*)^3(\alpha_1 + \alpha_1^*)(\alpha_1^2 - 4\alpha_1\alpha_1^* + \alpha_1^{*2}) \\
&+ 8\eta^3(\alpha_1 - \alpha_1^*)^3(i + 4\tau(\alpha_1^2 - \alpha_1^{*2})) + 4\eta^2(\alpha_1 - \alpha_1^*)^2\Big(-3 - 12i\tau(\alpha_1^2 - \alpha_1^{*2}) \\
&+ 16\tau^2(\alpha_1 - \alpha_1^*)^2(\alpha_1^2 + 4\alpha_1\alpha_1^* + \alpha_1^{*2}) - 16\eta\tau(\alpha_1 - \alpha_1^*)^2\Big(3\alpha_1^* - 32\tau^2\alpha_1^4\alpha_1^* \\
&+ 32\tau^2\alpha_1^3\alpha_1^{*2} + 8\tau\alpha_1^2\alpha_1^*(3i + 4\tau\alpha_1^{*2}) + \alpha_1(3 + 768i\tau^3\alpha_1^{*6})\Big).
\end{aligned}
$$

It is important to note that the third-order smooth positon solution can be deduced from the research in [58] by setting $\nu = 0$. By substituting this third-order smooth positon solution of the ccNLS Equation (13), along with the appropriate form of the modulated parameter $R(t)$, into Equation (7), we delve into an analysis of the underlying characteristics of the GP Equation (1).

Figure 4a–f present the condensate profiles of third-order smooth positons with a kink-like nonlinearity-modulated function $R(t) = R_0 + R_1 \tanh(R_2 t + R_3)$. By considering the initial parameters $R_0 = 1.25$, $R_1 = 0.01$, $R_2 = 1.05$, and $R_3 = 0.5$, an appropriate third-order positon profile is formed within the condensate density background, as shown in Figure 4a. Notably, a decrease in R_0 leads to a sudden rise in one of the subcrests, as demonstrated in Figure 4b for $R_0 = 0.85$. Furthermore, Figure 4c illustrates an increase in amplitude when changing the value of R_0 to 1.75. On the other hand, in Figure 4d, when the parameter R_1 is increased to 1.25, the positon tends to disappear within the condensate profile when $t < 0$. Interestingly, a reverse scenario occurs when $R_1 = -0.65$, resulting in

a higher peak in one of the profiles and an increased amplitude, as depicted in Figure 4e. Similarly, an increase in R_2 to 3.75 yields a compressed three-positon profile with the same amplitude as Figure 4a, as shown in Figure 4f.

(a)

(b)

(c)

(d)

(e)

(f)
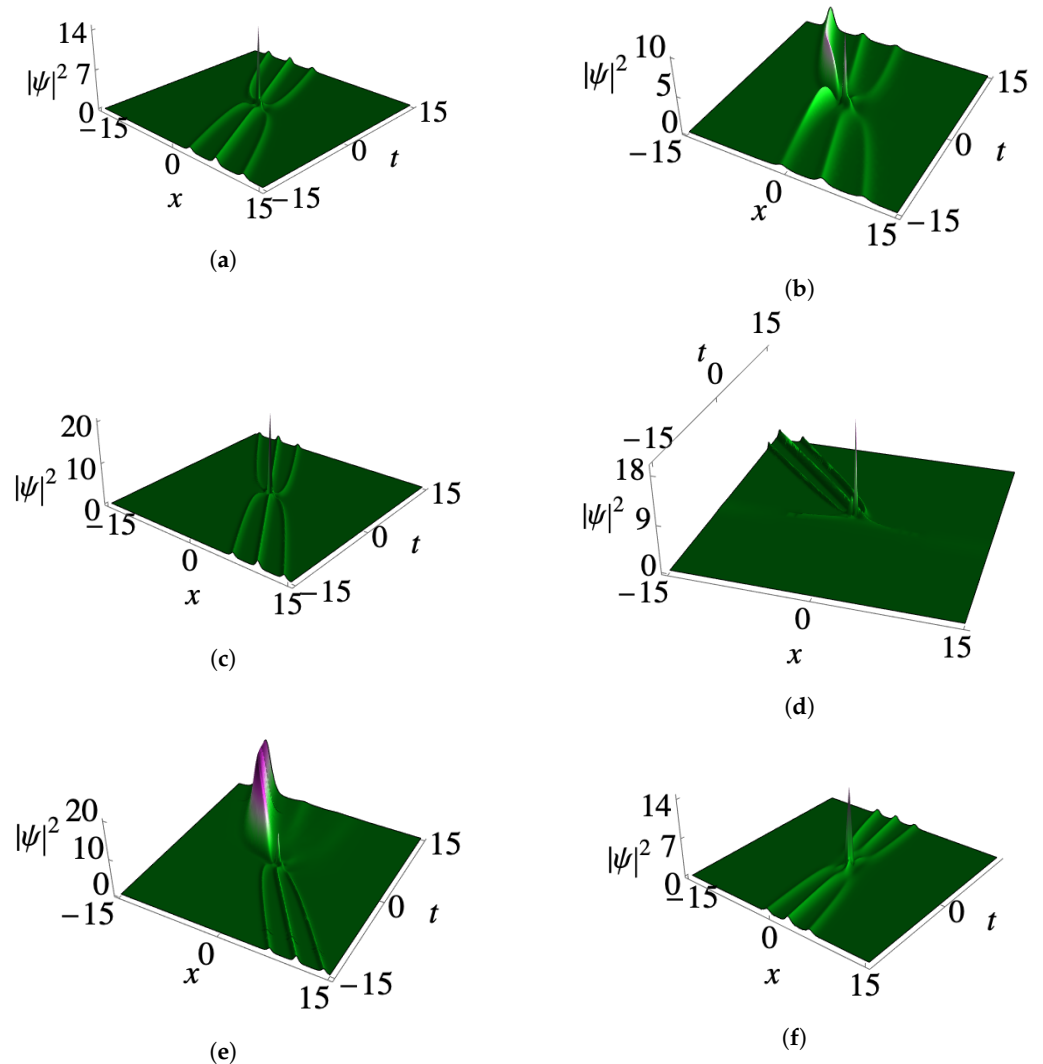
Figure 4. Density profile of third-order matter-wave smooth positons for (1) with $R(t) = R_0 + R_1$ tanh $(R_2 t + R_3)$. The parameters are (**a**) $R_0 = 1.25$, $R_1 = 0.01$, $R_2 = 1.05$, $R_3 = 0.5$; (**b**) $R_0 = 0.85$; (**c**) $R_0 = 1.75$; (**d**) $R_1 = 1.25$; (**e**) $R_1 = -0.65$; (**f**) $R_2 = 3.75$. In (**b**–**f**), the mentioned parameters are varied, while the remaining parameters are maintained as they are in (**a**). The other parameters are $\alpha_1 = 0.2 + 0.75i$, $\alpha_1^* = 0.2 - 0.75i$, $s_0 = 1.0$, and $b = 0.01$.
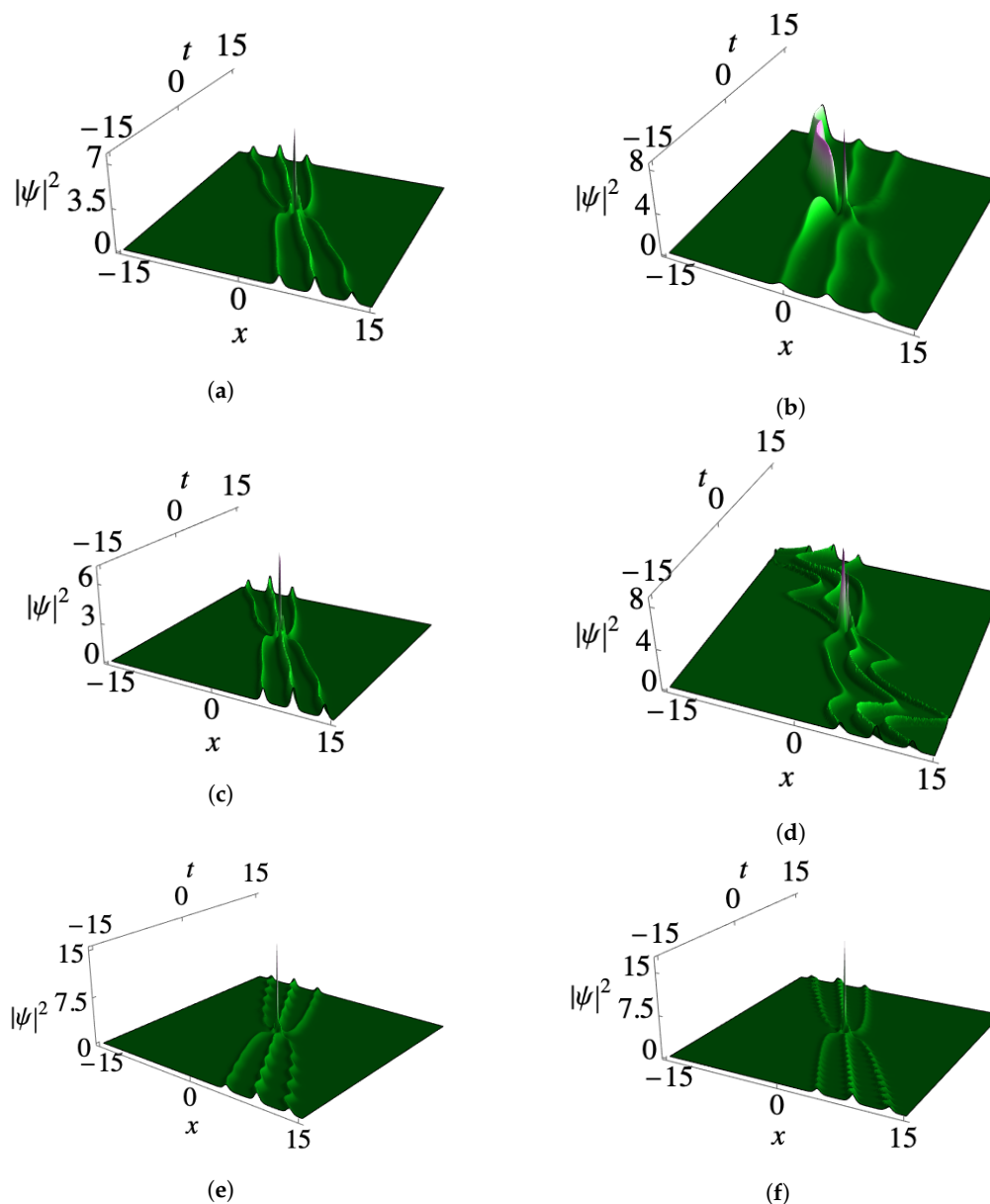
In Figure 5a–f, we show the density profiles of third-order matter-wave smooth positons for the sech-like nonlinearity-modulated function $R(t) = R_0 + R_1$ sech $(R_2 t + R_3)$ for the GP model (1). Employing the following initial parameters, namely, $R_0 = 1.25$, $R_1 = 0.01$, $R_2 = 1.05$, and $R_3 = 0.5$, we obtain the conventional smooth three-positon profile, as shown in Figure 5a. By adjusting R_0 to 1.85, the positon undergoes stretching, resulting in an enhanced amplitude, as depicted in Figure 5b. Similarly, when R_1 is modified to 1.5, the positon exhibits curvature in one of its wave crests, as seen in Figure 5c. Figure 5d illustrates a decrease in the soliton amplitude when R_1 is set to 0.35. However, no significant changes are observed in the smooth three-positon profile when altering the value of R_2 compared to Figure 5a. This observation is displayed in Figure 5e. Finally, for $R_0 = 1.85$ and $R_1 = 0.8$, the three-positon profile becomes compressed, which is accompanied by a decrease in its amplitude, as shown in Figure 5f.
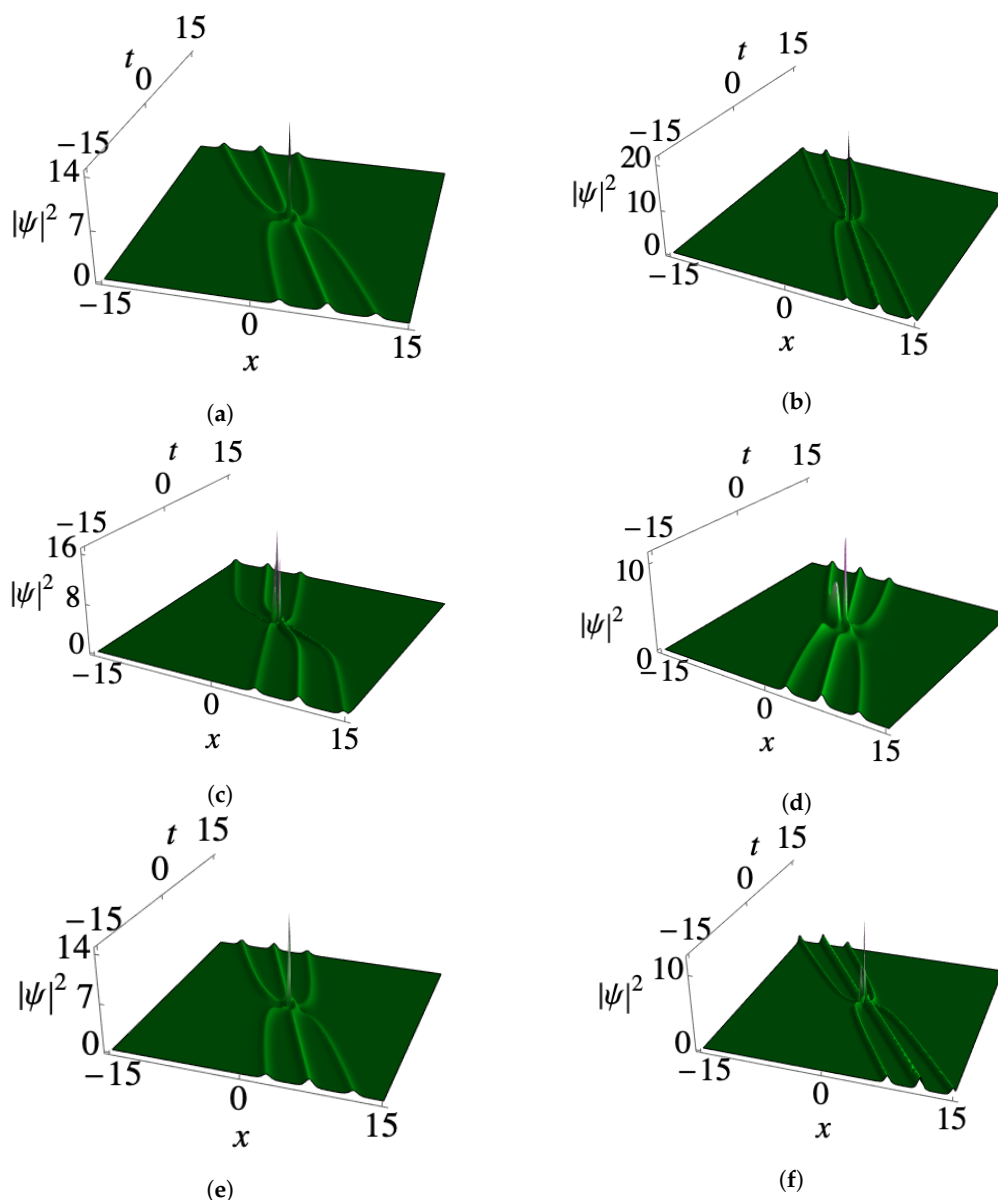
Figure 5. Density profile of third-order matter-wave smooth positons for (1) with nonlinearity-modulated function $R(t) = R_0 + R_1 \operatorname{sech}(R_2 t + R_3)$. The parameters are (**a**) $R_0 = 1.25$, $R_1 = 0.01$, $R_2 = 1.05$, $R_3 = 0.5$; (**b**) $R_0 = 1.85$; (**c**) $R_1 = 1.5$; (**d**) $R_1 = 0.35$; (**e**) $R_2 = 2.75$; (**f**) $R_0 = 1.85$, $R_1 = 0.8$. In (**b**–**f**), the mentioned parameters are varied, while the remaining parameters are maintained as they are in (**a**). The other parameters are the same as in Figure 4.

Finally, we investigate the density profiles of the third-order matter-wave smooth positon in one-component BECs utilizing a periodic nonlinearity-modulated function, denoted as $R(t) = R_0 + R_1 \sin(R_2 t + R_3)$. Setting the initial nonlinearity strengths as $R_0 = 1.5$, $R_1 = 0.05$, $R_2 = 0.85$, and $R_3 = 0.5$, we aim to obtain an appropriate periodic third-order smooth positon density profile, as illustrated in Figure 6a. Notably, in the results, a remarkable change occurs in the profile when the parameter R_0 is selected as 0.85, resulting in the formation of a sharp ascent on one side of the profile, as depicted in Figure 6b. Similarly, when we increase R_0 to 1.75, the profile returns to its original position, as displayed in Figure 6c. Furthermore, in Figure 6d, we observe that the periodicity of the positon density profiles increases when R_1 is set to 0.5. Moreover, raising the value of R_2 to 2.25 leads to an increase in the oscillation amplitude of the positon, as demonstrated in Figure 6e. Finally, when the value of R_2 is further increased to 5.25, we observe no change

in the positon amplitude, but there is a variation in the oscillation behavior, which is clearly depicted in Figure 6f.

(a)

(b)

(c)

(d)

(e)

(f)

Figure 6. Density profile of third-order matter-wave smooth positons for (1) with the nonlinearity-modulated function $R(t) = R_0 + R_1 \sin (R_2 t + R_3)$. The parameters are (**a**) $R_0 = 1.5$, $R_1 = 0.05$, $R_2 = 0.85$, $R_3 = 0.5$; (**b**) $R_0 = 0.85$; (**c**) $R_0 = 1.75$; (**d**) $R_1 = 0.5$; (**e**) $R_2 = 2.25$; (**f**) $R_2 = 5.25$. In (**b**–**f**), the mentioned parameters are varied, while the remaining parameters are maintained as they are in (**a**). The other parameters are the same as in Figure 4.

4. Conclusions

In our study, we have derived the second- and third-order matter-wave smooth positon solutions of the GP equation. These solutions capture the features of one-component BECs subjected to time-modulated nonlinearity (represented by the effective scattering lengths) and external harmonic trap potentials. Through a similarity transformation technique, we have mapped the time-modulated GP equation onto the ccNLS Equation, ensuring an integrability condition between the nonlinearity coefficient and the external trap potential. We have investigated three distinct forms of modulated nonlinearities: (i) kink-like, (ii) localized or sech-like, and (iii) periodic. By varying the parameters associated with the nonlinearity strength, we observed various nonlinear phenomena in the positon density

profiles. These phenomena include stretching, curving, oscillating, breathing, collapsing, amplification, and suppression. In the case of a kink-like modulated nonlinearity, the positon density profiles (represented by the second- and third-order matter-wave smooth positons) undergo stretching, while their amplitudes can be enhanced or suppressed. It is noteworthy that these profiles vanish for different time intervals, with disappearance occurring for $t < 0$ and $t > 0$ when the parameter R_2 takes positive and negative values, respectively. For localized or sech-type modulated nonlinearity, the density profiles of the positons become compressed and curved within the condensate density background. In the case of periodically modulated nonlinearity, the positons exhibit a periodic nature, and we observed an increase in periodicity as the nonlinearity strengths were adjusted. Our findings contribute to a deeper understanding of the behavior of matter-wave positons in BECs under different types of modulated nonlinearities. These results shed light on the intricate interplay between nonlinearity, external trapping potentials, and the corresponding effects on the density profiles of positons. The theoretical findings presented in this study, along with those presented in previous research, offer a valuable groundwork for experimental researchers to explore and validate the deformation of solitons/positons in $\mathcal{PT}$-symmetric systems with spatiotemporal modulation. These investigations can be extended to various fields, such as BECs and nonlinear optics, which are currently of great interest. Additionally, as a future direction, this theoretical study can be readily expanded to examine higher-order solitons, breathers, and rogue waves. It can also encompass the exploration of combined spatial and longitudinally varying trap potentials, nonlinear effects, and novel forms of $\mathcal{PT}$-symmetric potentials, potentially leading to the discovery of new applications.

References

1. Pitaevskii, L.P.; Stringari, S. *Bose-Einstein Condensation*; Clarendon: Oxford, UK, 2003.
2. Kevrekidis, P.G.; Frantzeskakis, D.J.R.; Carretero-Gonzlez, R. *Emergent Nonlinear Phenomena in Bose-Einstein Condensates*; Springer: Berlin/Heidelberg, Germany, 2008.
3. Lakshmanan, M.; Rajasekar, S. *Nonlinear Dynamics: Integrablity, Chaos and Patterns*; Springer: Berlin/Heidelberg, Germany, 2003.
4. Yang, J. *Nonlinear Waves in Integrable and Nonintegrable Systems*; SIAM: Philadelphia, PA, USA, 2010.
5. Ponomarenko, S.A.; Agrawal, G.P. Do solitonlike self-similar waves exist in nonlinear optical media? *Phys. Rev. Lett.* **2006**, *97*, 013901. [CrossRef]
6. Ponomarenko, S.A.; Agrawal, G.P. Optical similaritons in nonlinear waveguides. *Opt. Lett.* **2007**, *32*, 1659. [CrossRef]
7. Ponomarenko, S.A.; Agrawal, G.P. Interactions of chirped and chirp-free similaritons in optical fiber amplifiers. *Opt. Express* **2007**, *15*, 2963–2973. [CrossRef]
8. Serkin, V.N.; Hasegawa, A.; Belyaeva, T.L. Solitary waves in nonautonomous nonlinear and dispersive systems: Nonautonomous solitons. *J. Mod. Opt.* **2010**, *57*, 1456–1472. [CrossRef]
9. Luo, H.G.; Zhao, D.; He, X.G. Exactly controllable transmission of nonautonomous optical solitons. *Phys. Rev. A* **2009**, *79*, 063802. [CrossRef]
10. Shats, M.; Punzmann, H.; Xia, H. Capillary rogue waves. *Phys. Rev. Lett.* **2010**, *104*, 104503. [CrossRef]

11. Ganshin, A.N.; Efimov, V.B.; Kolmakov, G.V.; Mezhov-Deglin, L.P.; McClintock, P.V. Observation of an inverse energy cascade in developed acoustic turbulence in superfluid helium. *Phys. Rev. Lett.* **2008**, *101*, 065303. [CrossRef]
12. El-Tantawy, S.A.; Salas, A.H.; Albalawi, W. New Localized and Periodic Solutions to a Korteweg-de Vries Equation with Power Law Nonlinearity: Applications to Some Plasma Models. *Symmetry* **2022**, *14*, 197. [CrossRef]
13. Vudragović, D.; Balaž, A. Faraday and Resonant Waves in Dipolar Cigar-Shaped Bose-Einstein Condensates. *Symmetry* **2019**, *11*, 1090. [CrossRef]
14. Inouye, S.; Andrews, M.R.; Stenger, J.; Miesner, H.J.; Stamper-Kurn, D.M.; Ketterle, W. Observation of Feshbach resonances in a Bose-Einstein condensate. *Nature* **1998**, *392*, 151. [CrossRef]
15. Theis, M.; Thalhammer, G.; Winkler, K.; Hellwig, M.; Ruff, G.; Grimm, R.; Denschlag, J.H. Tuning the scattering length with an optically induced Feshbach resonance. *Phys. Rev. Lett.* **2004**, *93*, 123001. [CrossRef] [PubMed]
16. Malomed, B.A. *Soliton Management in Periodic Systems*; Springer: New York, NY, USA, 2006.
17. Wang, D.S.; Liu, J.; Wang, L. Non-autonomous matter-wave solitons in hybrid atomic-molecular Bose-Einstein condensates with tunable interactions and harmonic potential. *Phys. Lett. A* **2018**, *382*, 799–805. [CrossRef]
18. Halder, B.; Ghosh, S.; Basu, P.; Bera, J.; Malomed, B.; Roy, U. Exact solutions for solitary waves in a Bose-Einstein condensate under the action of a four-color optical lattice. *Symmetry* **2022**, *14*, 49. [CrossRef]
19. Bludov, Y.V.; Konotop, V.V.; Akhmediev, N. Matter rogue waves. *Phys. Rev. A* **2009**, *80*, 033610. [CrossRef]
20. Manikandan, K.; Muruganandam, P.; Senthilvelan, M.; Lakshmanan, M. Manipulating matter rogue waves and breathers in Bose-Einstein condensates. *Phys. Rev. E* **2014**, *90*, 062905. [CrossRef]
21. Wen, L.; Li, L.; Li, Z.-D.; Song, S.-W.; Zhang, X.-F.; Liu, W.M. Matter rogue wave in Bose-Einstein condensates with attractive atomic interaction. *Eur. Phys. J. D* **2011**, *64*, 473. [CrossRef]
22. Hacker, N.; Malomed, B.A. Nonlinear Dynamics of Wave Packets in Tunnel-Coupled Harmonic-Oscillator Traps. *Symmetry* **2021**, *13*, 372. [CrossRef]
23. Triki, H.; Choudhuri, A.; Qin, Z.; Biswas, A.; Alshomrani, A.S. Nonautonomous matter wave bright solitons in a quasi-1D Bose-Einstein condensate system with contact repulsion and dipole-dipole attraction. *Appl. Math. Comput.* **2020**, *371*, 124951. [CrossRef]
24. Sakaguchi, H.; Malomed, B. Nonlinear Management of Topological Solitons in a Spin-Orbit-Coupled System. *Symmetry* **2019**, *11*, 388. [CrossRef]
25. Zhao, L.C. Dynamics of nonautonomous rogue waves in Bose-Einstein condensate. *Ann. Phys.* **2013**, *73*, 329. [CrossRef]
26. He, J.S.; Charalampidis, E.G.; Kevrekidis, P.G.; Frantzeskakis, D.J. Rogue waves in nonlinear Schrödinger models with variable coefficients: Application to Bose-Einstein condensates. *Phys. Lett. A* **2014**, *378*, 577. [CrossRef]
27. Djoptoussia, C.; Tiofack, C.G.L.; Alim Mohamadou, A.; Kofane, T.C. Ultrashort self-similar periodic waves and similaritons in an inhomogeneous optical medium with an external source and modulated coefficients. *Nonlinear Dyn.* **2022**, *107*, 3833–3846. [CrossRef]
28. Xue, R.; Yang, R.; Jia, H.; Wang, Y. Novel bright and kink similariton solutions of cubic-quintic nonlinear Schrödinger equation with distributed coefficients. *Phys. Scr.* **2021**, *96*, 125230. [CrossRef]
29. Triki, H.; Jose, A.; Nithyanandan, K. Chirped self-similar localized pulses on a continuous wave background in presence of cubic-quintic nonlinearity and self-frequency shift. *Optik* **2022**, *70*, 169876. [CrossRef]
30. Ranjani, S.S.; Shreecharan, T.; Raju, T.S. Controllable behavior of self-similar matter waves in exotic transient trap variations. *Int. J. Theor. Phys.* **2023**, *62*, 15. [CrossRef]
31. Huo, K.; Shen, H. The self-similar brightlike darklike and W-shape solitons in inhomogeneous higher order nonlinear Schrödinger equation. *Optik* **2023**, *272*, 170314. [CrossRef]
32. Gubeskys, A.; Malomed, B.A.; Merhasin, I.M. Alternate Solitons: Nonlinearly managed one- and two-dimensional solitons in optical lattices. *Stud. Appl. Math.* **2005**, *115*, 255. [CrossRef]
33. Kartashov, Y.V.; Malomed, B.A.; Torner, L. Solitons in nonlinear lattices. *Rev. Mod. Phys.* **2011**, *83*, 247. [CrossRef]
34. Zhong, W.P.; Chen, L.; Belić, M.; Petrović, N. Controllable parabolic-cylinder optical rogue wave. *Phys. Rev. E* **2014**, *90*, 043201. [CrossRef]
35. Zhong, W.P.; Chen, L.; Belić, M. Breather solutions of the generalized nonlinear Schrödinger equation with spatially modulated parameters and a special external potential. *Eur. Phys. J. Plus* **2014**, *129*, 234. [CrossRef]
36. Konotop, V.V.; Yang, J.; Zezyulin, D.A. Nonlinear waves in $\mathcal{PT}$-symmetric systems. *Rev. Mod. Phys.* **2016**, *88*, 035002. [CrossRef]
37. Zezyulin, D.A.; Konotop, V.V. Nonlinear mode in the harmonic $\mathcal{PT}$-symmetric potential. *Phys. Rev. A* **2012**, *85*, 043840. [CrossRef]
38. Manikandan, K.; Sudharsan, J.B.; Senthilvelan, M. Nonlinear tunneling of solitons in a variable coefficients nonlinear Schrödinger equation with $\mathcal{PT}$-symmetric Rosen-Morse potential. *Eur. Phys. J. B* **2021**, *94*, 122. [CrossRef]
39. Oliinyk, A.; Yatsuta, I.; Malomed, B.; Yakimenko, A. Symmetry Breaking in Interacting Ring-Shaped Superflows of Bose-Einstein Condensates. *Symmetry* **2019**, *11*, 1312. [CrossRef]
40. Matveev, V.B. Generalized Wronskian formula for solutions of the KdV equations: First applications. *Phys. Lett. A* **1992**, *166*, 205–208. [CrossRef]
41. Matveev, V.B. Positon-positon and soliton-positon collisions: KdV case. *Phys. Lett. A* **1992**, *166*, 209–212. [CrossRef]
42. Matveev, V.B. Positons: Slowly Decreasing Analogues of Solitons. *Theor. Math. Phys.* **2002**, *131*, 483. [CrossRef]

43. Kedziora, D.J.; Ankiewicz, A.; Akhmediev, N. Second-order nonlinear Schrödinger equation breather solutions in the degenerate and rogue wave limits. *Phys. Rev. E* **2012**, *85*, 066601. [CrossRef]
44. Chow, K.W.; Lai, W.C.; Shek, C.K.; Tso, K. Positon-like Solutions of Nonlinear Evolution Equations in (2 + 1) Dimensions. *Chaos Solitons Fractals* **1998**, *9*, 1901–1912. [CrossRef]
45. Dubard, P.; Gaillard, P.; Klein, C.; Matveev, V.B. On multi-rogue wave solutions of the NLS equation and positon solutions of the KdV equation. *Eur. Phys. J. Spec. Top.* **2010**, *185*, 247–258. [CrossRef]
46. Stahlhofen, A.A. Positons of the modified Korteweg-de Vries equation. *Ann. Phys.* **1992**, *504*, 554–569. [CrossRef]
47. Maisch, H.; Stahlhofen, A.A. Dynamic properties of positons. *Phys. Scr.* **1995**, *52*, 228–236. [CrossRef]
48. Hu, H.C.; Liu, Y. New positon, negaton and complexiton solutions for the Hirota-Satsuma coupled KdV system. *Phys. Lett. A* **2008**, *372*, 5795–5798. [CrossRef]
49. Cen, J.; Correa, F.; Fring, A. Time-delay and reality conditions for complex solitons. *J. Math. Phys.* **2017**, *58*, 032901. [CrossRef]
50. Cen, J.; Correa, F.; Fring, A. Degenerate multi-solitons in the sine-Gordon equation. *J. Phys. A* **2017**, *50*, 435201. [CrossRef]
51. Xing, Q.; Wu, Z.; Mihalache, D.; He, J.S. Smooth positon solutions of the focusing modified Korteweg-de Vries equation. *Nonlinear Dyn.* **2017**, *89*, 2299–2310. [CrossRef]
52. Liu, W.; Zhang, Y.S.; He, J.S. Dynamics of the smooth positons of the complex modified KdV equation. *Waves Random Complex Media* **2018**, *28*, 203–214. [CrossRef]
53. Liu, S.Z.; Zhang, Y.S.; He, J.S. Smooth positons of the second-type derivative nonlinear Schrödinger equation. *Commun. Theor. Phys.* **2019**, *71*, 357–361. [CrossRef]
54. Song, W.; Xu, S.; Li, M.; He, J. Generating mechanism and dynamic of the smooth positons for the derivative nonlinear Schrödinger equation. *Nonlinear Dyn.* **2019**, *97*, 2135–2145. [CrossRef]
55. Yuan, F. The dynamics of the smooth positon and b-positon solutions for the NLS-MB equations. *Nonlinear Dyn.* **2020**, *102*, 1761–1771. [CrossRef]
56. Hu, A.; Li, M.; He, J. Dynamic of the smooth positons of the higher-order Chen-Lee-Liu equation. *Nonlinear Dyn.* **2021**, *104*, 4329–4338. [CrossRef]
57. Zhang, Z.; Yang, X.; Li, B. Soliton molecules and dynamics of the smooth positon for the Gerdjikov-Ivanov equation. *Appl. Math. Lett.* **2020**, *103*, 106168. [CrossRef]
58. Vishnu Priya, N.; Monisha, S.; Senthilvelan, M.; Rangarajan, G. Nth-order smooth positon and breather-positon solutions of a generalized nonlinear Schrödinger equation. *Eur. Phys. J. Plus* **2022**, *137*, 646. [CrossRef]
59. Monisha, S.; Vishnu Priya, N.; Senthilvelan, M.; Rajasekar, S. Higher order smooth positon and breather positon solutions of an extended nonlinear Schrödinger equation with the cubic and quartic nonlinearity. *Chaos Solitons Fractals* **2022**, *162*, 112433. [CrossRef]